

Observation of preferred heights in Pb nanoislands: A quantum size effect

Roberto Otero,* Amadeo L. Vázquez de Parga, and Rodolfo Miranda

Departamento de Física de la Materia Condensada and "Instituto Nicolás Cabrera," Universidad Autónoma de Madrid, 28049 Madrid, Spain

(Received 5 July 2002; published 3 September 2002)

Scanning-tunneling microscopy observation of Pb nanocrystals grown on Cu(111) indicates that in the equilibrium distribution of island heights some heights appear much more frequently than others. The simultaneous, local spectroscopic characterization allows us to relate this finding to the confinement of electrons within the islands: the "magic," preferred heights correspond to islands having a quantum well state far from the Fermi energy, while the "forbidden" heights turn out to be those that would have a quantum well state close to the Fermi level. The "magic" and "forbidden" heights can be predicted from the Fermi-surface geometry of bulk Pb.

DOI: 10.1103/PhysRevB.66.115401

PACS number(s): 73.21.Fg, 61.46.+w, 68.55.Jk

I. INTRODUCTION

Spatial confinement of electrons by a one-dimensional (1D) potential well results in discrete energy states, known as quantum well states (QWS's). By adjusting the physical dimensions of the confinement region, QWS's can be placed at the Fermi level [with the corresponding increase in the density of states (DOS)]. This is important because the DOS at the Fermi level triggers a number of electronic phase transitions (superconductivity, charge-density waves, lattice distortions, ferromagnetism, antiferromagnetism). For example, the (spin-polarized) QWS's play a decisive role in the oscillatory coupling of magnetic layers across nonmagnetic, metallic spacers.^{1,2} In magnetic/nonmagnetic trilayers, it has been found that when the nonmagnetic spacer thickness is such that there would be a maximum in the DOS at the Fermi level due to a QWS, the second magnetic layer orders antiferromagnetically with respect to the first one.² This lowers the symmetry of the system and eliminates the QWS at the Fermi energy, thereby decreasing the total energy of the system. Thus, one can say that the antiferromagnetic coupling is driven by the need to avoid the presence of a QWS at the Fermi level.

Due to the electronic states produced by the confinement, the total electronic energy will oscillate with the thickness of metallic films. If the contribution of the electronic energy to the total energy is significant, some sizes could be energetically more favorable than others. In fact, the energy associated to the confined motion of electrons was postulated to be important for the appearance of "magic" sizes in the formation of Na clusters³ in free space. The possibility of quantum size effects affecting morphology in thin films has also been reported for metallic islands on semiconductor substrates, i.e., a single "magic" height for Ag films on GaAs(110),⁴ and Ag (Refs. 5 and 6) and Pb (Refs. 7 and 8) on Si(111). It has been proposed that the competition between quantum confinement, charge spilling, and interface-induced Friedel oscillation defined the existence of critical/magical thicknesses in these cases.⁹ Recently, it has been reported that 5-monolayer (ML)-thick Ag films on Fe(100) are especially stable.¹⁰ In the theoretical model used it was concluded that the contribution of the electronic energy of the QWS associ-

ated to this particular film thickness has a significant contribution to the stability of the Ag film.

In this paper we report on the decisive influence of QWS's to dictate the heights observed in the equilibrium distribution of nanometer-high Pb islands grown on Cu(111). We explore a wide range of Pb coverage from 4 equivalent ML up to 22 equivalent ML. Both the height of the islands and their electronic structure are locally determined with scanning-tunneling microscopy (STM). We will demonstrate that the island heights most probable are those presenting a QWS placed far from the Fermi level, while those that only rarely appear have a QWS located close to the Fermi level. In other words, the islands rearrange their height to avoid the presence of QWS's at the Fermi level. Furthermore, we will show that the shape of the Fermi surface of Pb and, in particular, the nesting vectors, determine the distribution of heights found in our experiments.

II. EXPERIMENTAL PROCEDURES

The experiments have been carried out in an ultrahigh vacuum chamber containing a homemade STM, rear-view low-energy electron-diffraction optics, Auger spectroscopy, and facilities for ion sputtering, cooling the sample and depositing metals. The Cu(111) single crystal was electrochemically polished, sputter-annealed (500 eV, 800 K) for 5 min, and cooled down to 300 K. Pb was evaporated by electron bombardment with a deposition rate of 0.1 ML/min with the sample at room temperature. After the deposition the sample was flash-annealed to 400 K. The STM tips were made of electrochemically etched polycrystalline W and cleaned and characterized for spectroscopic measurements as described elsewhere.¹¹

III. STATISTICAL ANALYSIS OF ISLAND HEIGHTS

Depositing Pb on Cu(111) at 300 K and above¹² leads to a Stranski-Krastanov mode of growth,¹³ i.e., after the completion of the first monolayer 3D Pb islands grow on the surface. Figure 1 shows a representative image of this mode of growth. The characteristic lateral dimension of the islands is around 400–600 Å for our growth conditions. The islands

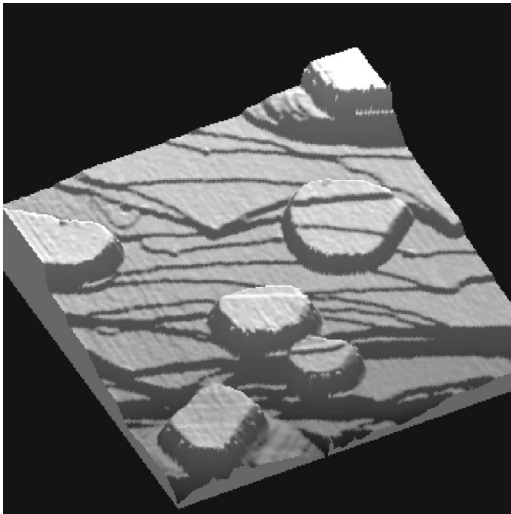


FIG. 1. STM topography of an area $3000 \times 3000 \text{ \AA}^2$ showing several Pb islands on a stepped Cu(111) surface. The image was taken at a sample bias of 1.2 V. The top surface of the Pb crystallites is atomically flat, but the steps of the substrate can still be recognized at the surface of the islands due to the difference in lattice parameter between Pb and Cu. The lateral dimension of the islands is 400–600 \AA .

are (111) oriented Pb nanocrystallites whose heights are always an integer number of Pb(111) interplanar distances (2.86 \AA). In large terraces of the substrate every Pb island has a unique height, while in regions of the sample with a high density of steps (i.e., in step bunches such as the one shown in Fig. 1), the islands may extend over several terraces of the substrate with their thickness changing by 1 ML from terrace to terrace. This shape has been termed an “atomic wedge.”¹⁴ The substrate steps crossed by the Pb islands can be recognized at the island surface due to the difference in the interplanar distance for lead (2.86 \AA) and copper (2.1 \AA) in the [111] direction. This difference produces a small step of 0.76 \AA at the island surface that allows us to unambiguously assign the thickness of Pb in every portion of each island.

The statistical distribution of island heights in a sample prepared with a given deposition rate and substrate temperature can be obtained through the analysis of several STM images recorded on different areas of the sample. The size of the images has been chosen to be $3000 \times 3000 \text{ \AA}^2$, that is, large enough to ensure that they show a statistically significant part of the film, while still allowing a clear identification of the island heights. It is also important to determine the possible influence of substrate steps in the observed height distribution. To this end four examples of the STM images, selected among those used to determine the island height distribution of one and the same sample, are displayed in Fig. 2. The images correspond to regions of the sample with different step density. In regions with less steps there are less islands, but they are larger. The local coverage varies slightly over the sample surface due to inhomogeneities during evaporation, but it does not depend on the step density. The heights of the Pb islands in atomic layers are also indicated in the figure. A casual inspection of the images reveals that

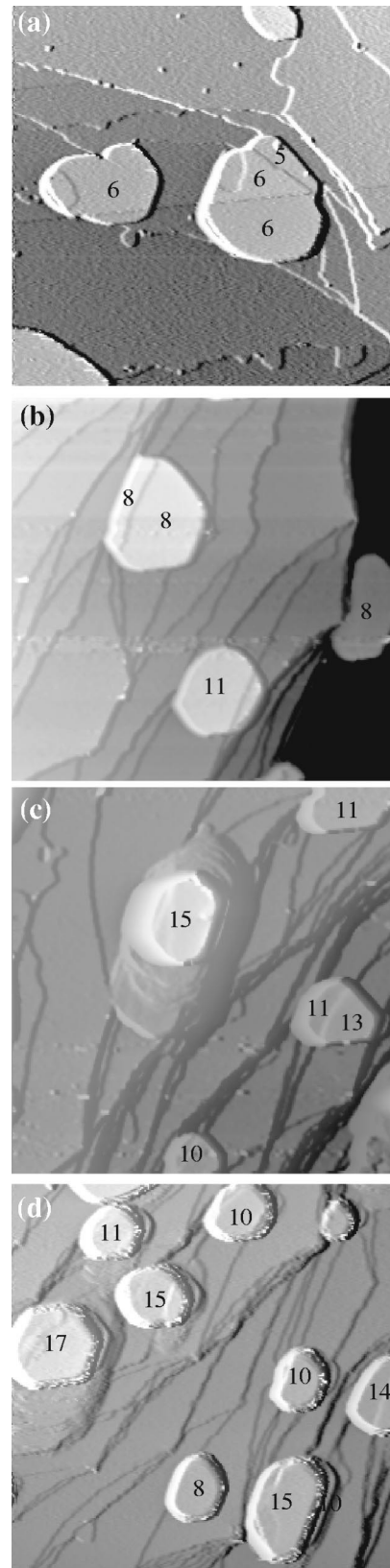


FIG. 2. Four representative STM images obtained in the same sample but in areas with a different local slope. The images are $3000 \times 3000 \text{ \AA}^2$, and a fraction of the differentiated image has been added to enhance the visibility of the substrate and island steps.

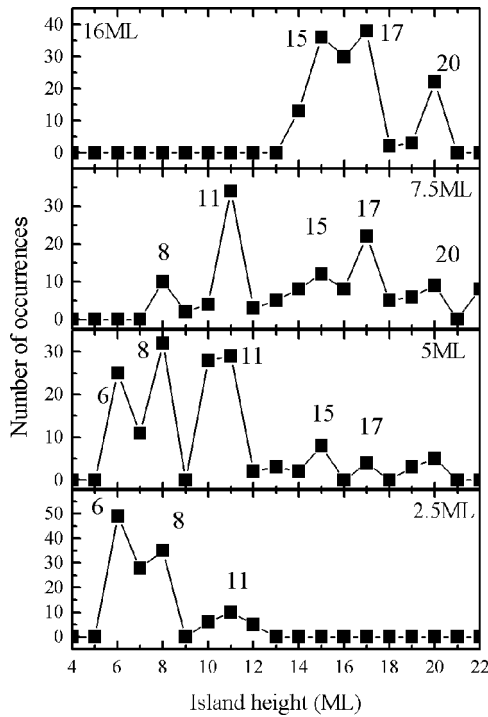


FIG. 3. Island height distributions (number of Pb islands with a given height) for different thicknesses of Pb deposited on Cu(111) at 300 K and annealed to 400 K. The data shown correspond to deposited nominal coverages of 2.5, 5, 7.5, and 16 ML, respectively.

some island heights seem to appear more frequently than others, regardless the local slope of the substrate. For instance, in the images of Fig. 2 several islands of 6, 8, 10–11, and 15 ML can be found, but not one appears with a height of 5, 9, 12, or 16 ML. It is evident that the detailed height distribution is different depending on the local concentration of steps, but in all cases only certain heights are observed.

To quantify this observation we counted the number of times that any given height appears on the surface without taking into account the size of the corresponding Pb island. In Fig. 3 we present the island height distribution for four films with increasing nominal coverage of Pb. In all cases *some island heights appear with higher probability than others*. For instance, there is a large number of islands with 6, 8, 11, 15, or 17 atomic heights, while those with 7, 9, or 12 are much less abundant. In fact the less frequent (“forbidden”) heights are only observed on narrow terraces corresponding to Pb islands that cross several substrate steps, sandwiched between the most commonly observed (“magic”) heights.

It seems that the presence of substrate steps forces the appearance of certain island heights that in a perfectly flat surface will be strictly forbidden. The existence of preferred or “magic” island heights is clearly revealed by weighting the island distribution with the area covered by every island height. In Fig. 4 we show the percentage of area covered by islands of any given height for increasing thicknesses of Pb. It is clear that certain thicknesses (5, 9, 12, 13, 14, and 18–19 ML) are forbidden, while 6, 8, 11, 15, 17, and 20 ML are strongly preferred. We have deposited films of Pb cover-

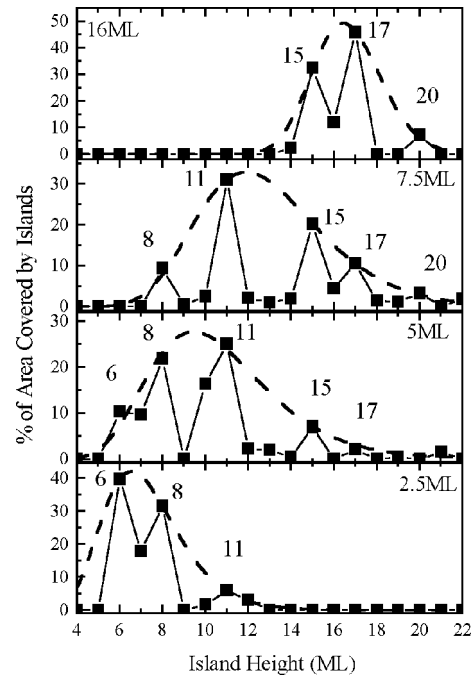


FIG. 4. Island height distributions (percentage of area covered by a given height) for Pb deposited on Cu(111) at 300 K and annealed to 400 K. The data shown correspond to deposited nominal coverages of 2.5, 5, 7.5, and 16 ML, respectively. Regardless of the coverage deposited, some island heights are strongly preferred, while others are almost never observed. The peaks corresponding to the “magically” preferred island heights are clearly resolved.

ing the thickness range from 2 to 20 equivalent ML. The existence of the same “magic” heights preferred for Pb islands in the equilibrium distribution was confirmed for films prepared with all different thicknesses.

IV. LOCAL DETECTION OF QWS'S BY SCANNING-TUNNELING SPECTROSCOPY

In the following we will demonstrate that the Pb islands behave as one-dimensional quantum wells along the [111] direction, where the electronic states are quantized. The effective depths of the wells is given by the local height of the island. The lateral dimensions of the islands (or even the terraces within a given island) are too large to produce lateral confinement. The *s-p* electrons of Pb around the Fermi energy are completely confined within the islands in the perpendicular (111) direction, by the vacuum barrier (Pb work function) and the Cu bulk band gap, respectively. The confinement induces the discretization of the Pb *sp* band and the corresponding QWS's can be detected locally by scanning-tunneling spectroscopy.^{14,15} Figure 5(a) shows representative dI/dV - V curves recorded at 300 K with the STM tip placed on top of Pb islands of varying height. The peaks in a given spectrum correspond to the different QWS's associated to the thickness of the Pb island. The position in energy of the QWS's do not depend on the lateral size of the island, only on its height. The QWS spectra are independent of the tip sample surface in the range used. The tick marks reflect the calculated energy positions of the QWS's, accurately pre-

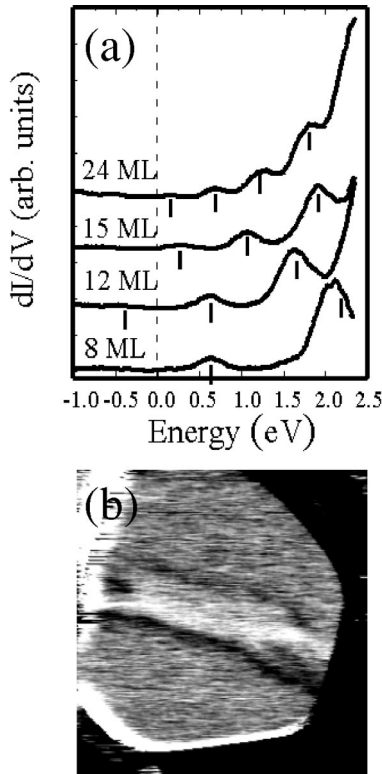


FIG. 5. (a) Set of measurements of tunneling conductance versus sample voltage recorded at constant height above selected Pb islands deposited on Cu(111). Notice the evolution of the quantized energy levels with the island height. The tick marks indicate the QWS's calculated for an infinite quantum well of the given thickness; (b) spectroscopic image $700 \times 700 \text{ \AA}^2$ of a Pb island containing several quantum wells. The dc voltage is tuned to a QWS of the central stripe (1.15 V). This image was acquired by adding an ac signal of 60 mV and 1.1 kHz.

dicted down to 4-ML-high islands by a simple, one-dimensional, infinitely high potential well model.¹⁵ The energy levels can also be described with more realistic phase accumulation models, taking into account the scattering properties of the Pb/Cu and the Pb/vacuum interfaces, but in this case the position of the scattering planes must be slightly shifted with respect to the interfaces, as has been discussed elsewhere.¹⁵

Figure 5(b) shows a spectroscopic image of the empty states recorded on top of one of the islands covering several terraces of the substrate. The image has been taken with a bias voltage tuned to a QWS of the central stripe. That well, thus, appears bright, while those adjacent with a thickness corresponding to 1 ML more or less appear darker since in the chosen energy window no QWS's exist. The image proves that, even when the islands extend over several terraces of the substrate and, then, present several atomic thicknesses, each island can be considered as an array of independent quantum wells as long as the lateral size of each terrace is larger than the Fermi wavelength of Pb. The large difference in energy between the QWS's of wells whose thicknesses differ by one layer (e.g., 0.21, 1.15, and 2.1 eV versus -0.38 , 0.65 , and 1.65 eV) results in no mixing of states even in the same island.

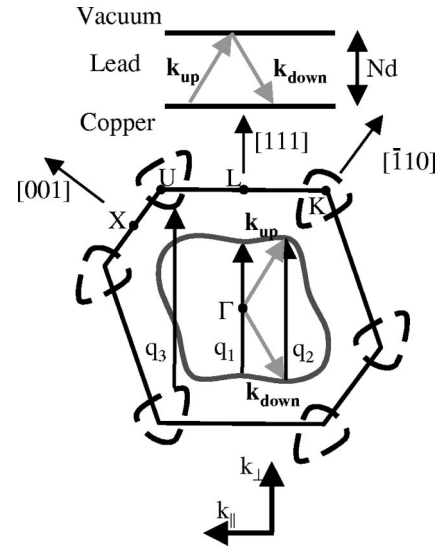


FIG. 6. Cut of the Fermi surface of Pb in the (111) plane (light gray). The three nesting vectors along the (111) direction are shown as thick arrows. The upper diagram shows schematically that under elastic reflection at the interfaces the perpendicular momentum transfer must link two points of the constant energy surface. Due to the confinement, the perpendicular momentum transfer is quantized.

V. ENERGETICS OF THE QWS'S AND THE NESTING VECTORS OF THE FERMI SURFACE

The total energy of the Pb islands contains a term given by the electronic energy of the occupied QWS's. This contribution could outweigh the elastic energy and, eventually, dictate the size distribution of the islands. The electronic energy of the occupied QWS's will be maximized whenever a QWS is placed right at the Fermi energy and it will decrease as the QWS passes above the Fermi level. Accordingly, the “magic” heights would be those of islands which present a QWS well separated from the Fermi level and the “forbidden” heights of islands with a QWS close to the Fermi energy. In order to qualify this suggestion, it is necessary to predict the actual heights of the Pb islands that will present a QWS located at the Fermi level. This can be done by means of the *nesting* vectors of the Fermi surface of Pb.¹⁶ The confinement of the electrons inside the islands quantizes their perpendicular momentum to a series of discrete values given by $k_n = n\pi/Nd$, with N being the number of Pb layers, d the interlayer distance, and n the (integer) quantum number.¹⁵ The DOS at the Fermi level and the total electronic energy will present a maximum due to the presence of a QWS whenever an n value satisfies $k_F = k_n$.

In Fig. 6 we show a cut of the calculated¹⁷ Fermi surface of bulk Pb along [111] displaying the nesting vectors and a schematic diagram showing that $q_{nesting}$ coincides with the first Brillouin-zone representation of $2k_{F,\perp}$. The hole surface in the second zone is indicated by the solid gray line, while the dashed gray line indicates the electron pockets in the third zone. Then, the island heights (Nd) with a maximum in the DOS at the Fermi level will be given by

$$N = \frac{2\pi}{q_{nesting}d} n. \quad (1)$$

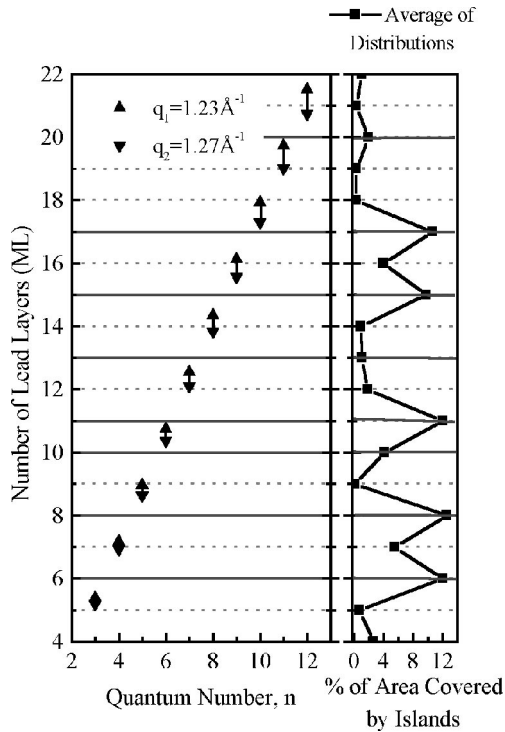


FIG. 7. (a) Left panel: The triangles indicate the Pb island heights, in number of layers, N , which would have a QWS at the Fermi energy according to Eq. (1). The heights are calculated for the different quantum numbers n and the two relevant nesting vectors of the bulk Fermi surface of Pb. (b) Right panel: Average of the distributions for different coverages. Notice that the “magic” island heights correspond to those that do not present an occupied QWS close to the Fermi energy. On the other hand, whenever the predicted values (triangles) come close to an integer value of Pb layers, the corresponding island is strongly suppressed in the observed distribution.

The magnitude of these three nesting vectors is 1.23, 1.27, and 1.79 \AA^{-1} , respectively. The nesting vector q_1 (1.23 \AA^{-1}) at \mathbf{k}_{\parallel} close to zero corresponds to the QWS detected by tunneling spectroscopy. These kind of QWS’s could also be detected by angle-resolved ultraviolet photoemission spectroscopy (ARUPS) at normal emission.¹⁸ The nesting vectors at nonzero parallel momentum, q_2 (1.27 \AA^{-1}) and $q_3 = 1.71 \text{ \AA}^{-1}$, give rise to QWS not seen by tunneling spectroscopy, but detectable by ARUPS with k_{\parallel} different from zero.¹⁹ The nesting vector q_2 will give almost the same periodicity in the DOS at the Fermi level and in the total electronic energy as q_1 , while the nesting vector q_3 will contribute little to the electronic energy due to the curvature of the Fermi surface at the connected points.

In Fig. 7 we plot the values of N corresponding to Eq. (1) for different values of the quantum number, n , and for the two nesting vectors that contribute more to the total electronic energy. Whenever N becomes an integer for some value of the quantum number, n , the density of states at the

Fermi level will present a maximum due to a QWS. We see that for $N=6, 8, 10, 11, 15, 17$, and 20 layers, there is no quantum number that yields a QWS close to the Fermi level. These are precisely the “magic” heights permitted for the Pb islands, as shown in the average distribution of island heights depicted in the right panel of Fig. 7. On the contrary, there are almost no islands with 5, 9, 12, 14, 18, 19, and 21 layers, where one or more QWS’s are predicted to be present at the Fermi energy. *The heights most frequently observed are those where the QWS’s are not close to the Fermi level, while for every thickness strongly suppressed, at least one of the nesting vectors satisfies Eq. (1), i.e., a quantum well state would be located at E_F .* This suggests that the system structurally rearranges itself to minimize the total energy, avoiding the islands with these numbers of layers.

VI. CONCLUSIONS

In conclusion, we have observed that certain island heights on films of Pb deposited on a Cu(111) surface are strongly preferred while some others are almost completely suppressed. The local, and simultaneously recorded topographic and spectroscopic data allow us to conclude that the Pb nanocrystallites rearrange their height to avoid the energetically unfavorable situation of having a subband of QWS and, thus, a high DOS, at the Fermi level. The energy contribution of the QWS influences the resulting island morphology. The QWS’s with parallel components of the momentum close to zero are directly detected by scanning-tunneling spectroscopy, while the others are deduced from the nesting vectors of the Pb Fermi surface. In all the range explored the “magic” heights can be accurately predicted from the nesting vectors of the Fermi surface of Pb. This constitutes the first direct experimental evidence of the influence of QWS’s in determining the equilibrium size of nanocrystals. This experimental example of stable, “magic” heights in nanoislands (and possibly films) controlled by electronic states originated by the 1D confinement, namely, the quantum well states, extends previous notions on the role of the confined motion of electrons in determining “magic” sizes in nanoclusters³ (3D confinement) and nanowires²⁰ (2D confinement). In both cases, geometric structures minimizing the energies of the occupied states relative to the Fermi level seem to be preferred. This “electronic-controlled” mode of growth could have implications for the future wave-function engineering design of stable nanometer-scale materials and devices.

ACKNOWLEDGMENTS

This work has been financed by the Dirección General de Investigación, Ciencia y Tecnología (DGICYT) with Grant No. BFM2001-0174 and by the Consejería de Educación from the Comunidad de Madrid with Grant No. 07N/0055/2001.

- *Present address: CAMP and Department of Physics and Astronomy, University of Aarhus, DK-8000 Aarhus C, Denmark. Electronic address: roberto@phys.au.dk
- ¹A. Cebollada, R. Miranda, C.M. Schneider, P. Schuster, and J. Kirschner, *J. Magn. Magn. Mater.* **102**, 25 (1991).
- ²J.E. Ortega and F.J. Himpsel, *Phys. Rev. Lett.* **69**, 844 (1992).
- ³W.D. Knight, K. Clemenger, W.A. de Heer, W.A. Saunders, M.Y. Chou, and M.L. Cohen, *Phys. Rev. Lett.* **52**, 2141 (1984).
- ⁴A.R. Smith, K.-J. Chao, Q. Niu, and C.-K. Shih, *Science* **273**, 226 (1996).
- ⁵L. Gavioli, K.R. Kimberlin, M.C. Tringides, J.F. Wendelken, and Z. Zhang, *Phys. Rev. Lett.* **82**, 129 (1999).
- ⁶L. Huang, S.J. Hay, and J.H. Weaver, *Surf. Sci.* **416**, L1101 (1998).
- ⁷V. Yeh, L. Berbil-Bautista, C.Z. Wang, K.M. Ho, and M.C. Tringides, *Phys. Rev. Lett.* **85**, 5158 (2000).
- ⁸W.B. Su, S.H. Chang, W.B. Jian, C.S. Chang, L.J. Chen, and T.T. Tsong, *Phys. Rev. Lett.* **86**, 5116 (2001).
- ⁹Z. Zhang, Q. Niu, and C.-K. Shih, *Phys. Rev. Lett.* **80**, 5381 (1998).
- ¹⁰D.A. Luh, T. Miller, J.J. Paggel, M.Y. Chou, and T.-C. Chiang, *Science* **292**, 1131 (2001).
- ¹¹A.L. Vázquez de Parga, O. S. Herman, R. Miranda, A. Levy Yeyati, N. Mingo, A. Martin Rodero, and F. Flores, *Phys. Rev. Lett.* **80**, 357 (1998).
- ¹²This is in opposition to the nearly layer-by-layer growth mode of the same system at lower temperatures described by B.J. Hinch, C. Koziol, J. P. Toennies, and G. Zhang, *Europhys. Lett.* **10**, 341 (1989).
- ¹³J. Camarero, J. Ferren, V. Cros, L. Gomez, A.L. Vazquez de Parga, J.M. Gallego, J.E. Prieto, J.J. de Miguel, and R. Miranda, *Phys. Rev. Lett.* **81**, 850 (1998).
- ¹⁴I.B. Altfeder, K.A. Matveev, and D.M. Chen, *Phys. Rev. Lett.* **78**, 2815 (1997).
- ¹⁵R. Otero, A.L. Vázquez de Parga, and R. Miranda, *Surf. Sci.* **447**, 143 (2000).
- ¹⁶M.D. Stiles, *Phys. Rev. B* **48**, 7238 (1993).
- ¹⁷J.R. Anderson and J.A.V. Gold, *Phys. Rev.* **139**, 1459 (1965).
- ¹⁸T.-C. Chiang, *Surf. Sci. Rep.* **39**, 181 (2000).
- ¹⁹P. Segovia, E.G. Michel, and J.E. Ortega, *Phys. Rev. Lett.* **77**, 3455 (1996).
- ²⁰A.I. Yanson, I.K. Yanson, and J.M. van Ruitenbeek, *Nature (London)* **400**, 144 (1999).